THE BUFFER MECHANISM FOR MULTI-STEP INFORMATION REASONING IN LANGUAGE MODELS

Zhiwei Wang[1,2], **Yunji Wang**[1,2], **Zhongwang Zhang**[1,2], **Zhangchen Zhou**[1,2],
Hui Jin[4], **Tianyang Hu**[4], **Jiachen Sun**[4], **Zhenguo Li**[4], **Yaoyu Zhang**[1,2], **Zhi-Qin John Xu**[1,2,3*]

[1] Institute of Natural Sciences, MOE-LSC, Shanghai Jiao Tong University
[2] School of Mathematical Sciences, Shanghai Jiao Tong University
[3] Key Laboratory of Marine Intelligent Equipment and System, Ministry of Education
[4] Huawei Noah's Ark Lab

October 16, 2024

ABSTRACT

Large language models have consistently struggled with complex reasoning tasks, such as mathematical problem-solving. Investigating the internal reasoning mechanisms of these models can help us design better model architectures and training strategies, ultimately enhancing their reasoning capability. In this study, we constructed a symbolic dataset to investigate the mechanisms by which Transformer models employ vertical thinking strategy based on their inherent structure and horizontal thinking strategy based on Chain of Thought to achieve multi-step reasoning. We introduced the concept of buffer mechanism: the model stores various information in distinct buffers and selectively extracts them through the query-key matrix. We proposed a random matrix-based algorithm to enhance the model's reasoning ability, resulting in a 75% reduction in the training time required for the GPT-2 model to achieve generalization capability on the PrOntoQA dataset. These findings provide new insights into understanding the mechanisms of large language models.

1 Introduction

In recent years, LLMs have emerged and demonstrated remarkable capability across various tasks (Vaswani et al., 2017; Liu et al., 2018; Devlin et al., 2018; Radford et al., 2019; Touvron et al., 2023; OpenAI, 2023). These models have shown impressive in-context learning abilities (Brown et al., 2020; Dong et al., 2022; Garg et al., 2022) and have been applied to logical reasoning problems, such as matching top human contestants at the International Mathematical Olympiad (IMO) level (Trinh et al., 2024) and solving math problems (Davies et al., 2021).

However, even the most advanced models still struggle with complex reasoning tasks, which indicates the ability of LLMs to handle multi-step logical reasoning remains constrained. To truly enhance the reasoning capability of LLMs, it is crucial to investigate their intrinsic mechanisms.

Multi-step reasoning tasks encompass a broad concept, typically referring to the ability of a model to synthesize numerous complex conditions to answer questions. Here, we consider a representative class of syntactic structures within multi-step reasoning tasks: a sentence that includes both the question and sufficient known information to answer it. For example, "Given: `[A]`→`[B]`...`[B]`→`[C]`..., Question: 2-step reasoning starting from `[A]`", where "..." represents other textual content unrelated to logical reasoning. The answer to this question is "`[C]`". When a sentence contains only one logical reasoning step, it is often handled by the so-called induction head in Transformer (Brown et al., 2020; Olsson et al., 2022). However, multi-step reasoning is not merely a linear accumulation of multiple induction heads but involves more complex mechanisms.

---

*Corresponding author: xuzhiqin@sjtu.edu.cn

Question: We have established the following reasoning rules: (1) [a] to [b] represents that condition [a] can derive condition [b]. (2) The sequence [a] to [b] | [b] to [c] indicates that the 2-step reasoning result of [a] is [c]. For the following reasoning chain:

[e] to [i] | [r] to [w] | [n] to [a] | [o] to [p] | [i] to [r] | [p] to [e] | [w] to [p] | [x] to [i]

Please answer directly: What is the 4-step reasoning result of [w]? (only return the answer)

GPT-4o			GPT-4			Claude 3 Opus		
1. e	4. e	7. a	1. e	4. e	7. e	1. i	4. i	7. a
2. a	5. r ✓	8. e	2. c	5. r ✓	8. e	2. a	5. i	8. a
3. e	6. r ✓	9. n	3. e	6. e	9. e	3. i	6. i	9. i

Figure 1: Failure cases of multi-step reasoning in LLM. The correct answer is [r] (Since [w] $\rightarrow$ [p] $\rightarrow$ [e] $\rightarrow$ [i] $\rightarrow$ [r]). We tested each model 9 times.

Large models employ two primary strategies for logical reasoning. The first, known as the *Vertical Thinking Strategy (VTS)*, outputs reasoning results in a single forward based on their inherent structure. This approach is efficient but demands a high level of intelligence from the model itself. As shown in Fig. 1, current large models exhibit significant limitations in their vertical thinking capability. Another relatively less efficient approach is the *Horizontal Thinking Strategy (HTS)*, such as Chain of Thought (CoT) (Wei et al., 2022; Kojima et al., 2022) and Tree of Thought (ToT) (Yao et al., 2024), Diagram of Thought (DoT) (Zhang et al., 2024a). This strategy substantially enhances the model's reasoning performance. All models can produce the correct answers for tasks depicted in Fig. 1 with the help of CoT. Considering the strengths and weaknesses of these two strategies, the ideal approach should combine both: decomposing problems into several coarse-grained subproblems (HTS) and applying the VTS to each subproblem. Thus, researching how to improve vertical thinking capability and understanding why horizontal thinking strategy can significantly enhance model reasoning ability are both crucial.

In this work, we investigate the performance of Transformer models on a symbolic multi-step reasoning dataset. Our work aims to uncover these mechanisms and provide insights into how Transformer processes and integrates logical information across multiple layers to perform multi-step reasoning, which can help develop more effective strategies for improving their multi-step reasoning abilities. Specifically, we found that Transformers utilize a ***Buffer Mechanism*** when engaging in complex reasoning. The model stores different intermediate results in separate buffers, allowing for quick retrieval as needed. We elaborate on how the model leverages this buffer mechanism for vertical thinking and we explain why horizontal thinking strategy can significantly enhance the model's multi-step reasoning capability from the perspective of the buffer mechanism. Finally, based on this understanding, we propose a method to enhance the model's reasoning abilities, resulting in a 75% reduction in the cost of generalization for the GPT-2 model on the question-answering dataset PrOntoQA (Saparov & He, 2022). The concept of "buffer" or similar concepts has also been mentioned in other works (Reddy, 2023; Bietti et al., 2024; Elhage et al., 2021). Our work provides a detailed description of the concept of buffer and applies this mechanism to enhance model performance.

The main contributions of this work are as follows:

- We discover the buffer mechanism employed by language models during the reasoning process and provided a detailed analysis of the model's internal thinking process for vertical and horizontal thinking from the perspective of the buffer.

- We propose a method to enhance the model's reasoning capability, significantly improving data utilization efficiency in logical reasoning datasets.

Our research deepens the understanding of the reasoning mechanisms in Transformer models and provides new perspectives for further enhancing their reasoning capability. The insights gained from this study can contribute to the design of more efficient reasoning models and the exploration of reasoning mechanisms in general artificial intelligence systems.

2 Reasoning Dataset and Transformer Model

Dataset. To understand the mechanism of multi-step reasoning in Transformers, we design an abstract symbolic multi-step reasoning task. As shown in Fig. 2, reasoning chains are serialized into a sequence. Every two tokens in the sentence represent a reasoning relation. The last token is the reasoning start token, and the label is the reasoning result with a fixed-step reasoning starting from the starting point.
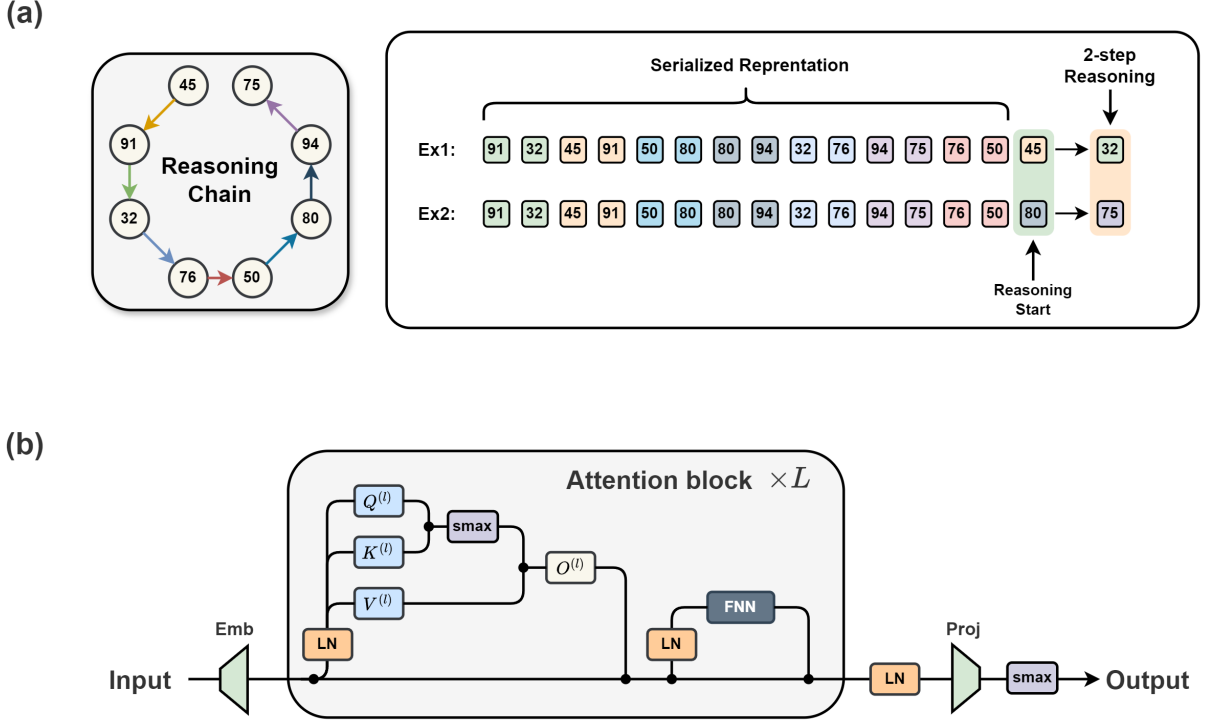

Figure 2: Illustration of the dataset and Transformer structure.

Transformer Model. We employ a decoder-only Transformer. Given an input sequence $\boldsymbol{X}^{\text{in}} \in \mathbb{R}^{n \times d}$, where n is the sequence length and d is the dictionary size, the model first applies an embedding layer (target embedding and position embedding) to obtain the input representation $\boldsymbol{X}^{(1)} = \boldsymbol{X}_{tgt} + \boldsymbol{X}_{pos} \in \mathbb{R}^{n \times d_m}$. The single-head attention in each layer is computed as follows:

$$\mathcal{A}^{(l)}(\boldsymbol{X}) = \sigma \left(\frac{\text{mask}(\boldsymbol{X}\boldsymbol{W}^{q(l)}\boldsymbol{W}^{k(l),\mathsf{T}}\boldsymbol{X}^{\mathsf{T}})}{\sqrt{d_k}} \right), \quad \boldsymbol{X}^{\text{qkv}(l)} = \mathcal{A}^{(l)}(\bar{\boldsymbol{X}}^{(l)})\bar{\boldsymbol{X}}^{(l)}\boldsymbol{W}^{v(l)}\boldsymbol{W}^{o(l)},$$

where σ takes the softmax operator, and $\bar{\boldsymbol{X}}^{(l)} = \text{Layernorm}(\boldsymbol{X}^{(l)})$. For simplicity of expression, we will abbreviate $\boldsymbol{W}^{q(l)}\boldsymbol{W}^{k(l),\mathsf{T}}$ as $\boldsymbol{W}^{qk(l)}$ and $\boldsymbol{W}^{v(l)}\boldsymbol{W}^{o(l),\mathsf{T}}$ as $\boldsymbol{W}^{vo(l)}$ in the following text. The output of the l-th layer is obtained as:

$$\boldsymbol{X}^{\text{ao}(l)} = \boldsymbol{X}^{(l)} + \boldsymbol{X}^{\text{qkv}(l)}, \quad \boldsymbol{X}^{(l+1)} = f^{(l)}(\bar{\boldsymbol{X}}^{\text{ao}(l)}) + \boldsymbol{X}^{\text{ao}(l)},$$

where $f^{(l)}(\cdot)$ represents the feedforward neural network of l-th layer. The final output (in the form of token indices within the vocabulary) is obtained as:

$$\boldsymbol{Y} = argmax(\sigma(\bar{\boldsymbol{X}}^{(L)}\boldsymbol{W}^p)) \in \mathbb{R}^n. \tag{1}$$

In Distribution and Out of Distribution Data. With the settings of our dataset, if the model truly understands the underlying logic patterns, it should be able to find the correct answer to the sentence, even if this sentence has tokens that have never been encountered during the training. Therefore, we divided the data into two parts: in-distribution (ID) and out-of-distribution (OOD). Specifically, we define $\text{token}_{\text{ID}} \in [20, 100]$ and $\text{token}_{\text{OOD}} \in [0, 120] \setminus [20, 100]$. In-distribution data ($\text{Train}_{\text{ID}}$ and Test_{ID}) is defined as sentences composed entirely of token_{ID}, while out-of-distribution data (Test_{OOD}) consists of sentences containing one $\text{token}_{\text{OOD}}$, which happens to be the previous reasoning step of label.

For the in-distribution data, we split the training set (Train$_{\text{ID}}$) and test set (Test$_{\text{ID}}$) according to the following rules: for the serialized reasoning chain [x$_1$][x$_2$]$\cdots$[x$_n$] of the training set, all tokens satisfy the following condition:

$$x_{2i} - x_{2i-1} \pmod{m} \in G. \tag{2}$$

For the reasoning chains in the test set, all tokens satisfy:

$$x_{2i} - x_{2i-1} \pmod{m} \in \{1, \cdots, m\} \backslash G, \tag{3}$$

where we take $m = 5$ and $G = \{0, 1, 4\}$ in this study. Under this setting, we ensure that each binary logical pair in the testing set has not previously appeared in the training set. Therefore the Transformer is performing in-context learning (Brown et al., 2020; Olsson et al., 2022), as each reasoning pair is not seen during in-weight learning.

3 Buffer Mechanism and Vertical Thinking Strategy

In this section, we examine the mechanism by which the Transformer model employs vertical thinking strategy for multi-step reasoning. We discovered that when the number of layers exceeds the number of reasoning steps, the Transformer's logic circuit of vertical thinking can be depicted in Fig. 3. The first layer facilitates the fusion of token information at odd and even positions. In each subsequent layer, which we refer to as the reasoning layer, the token at the last position attends to the token carrying the next reasoning result based on existing reasoning result, thereby accomplishing one-step reasoning.
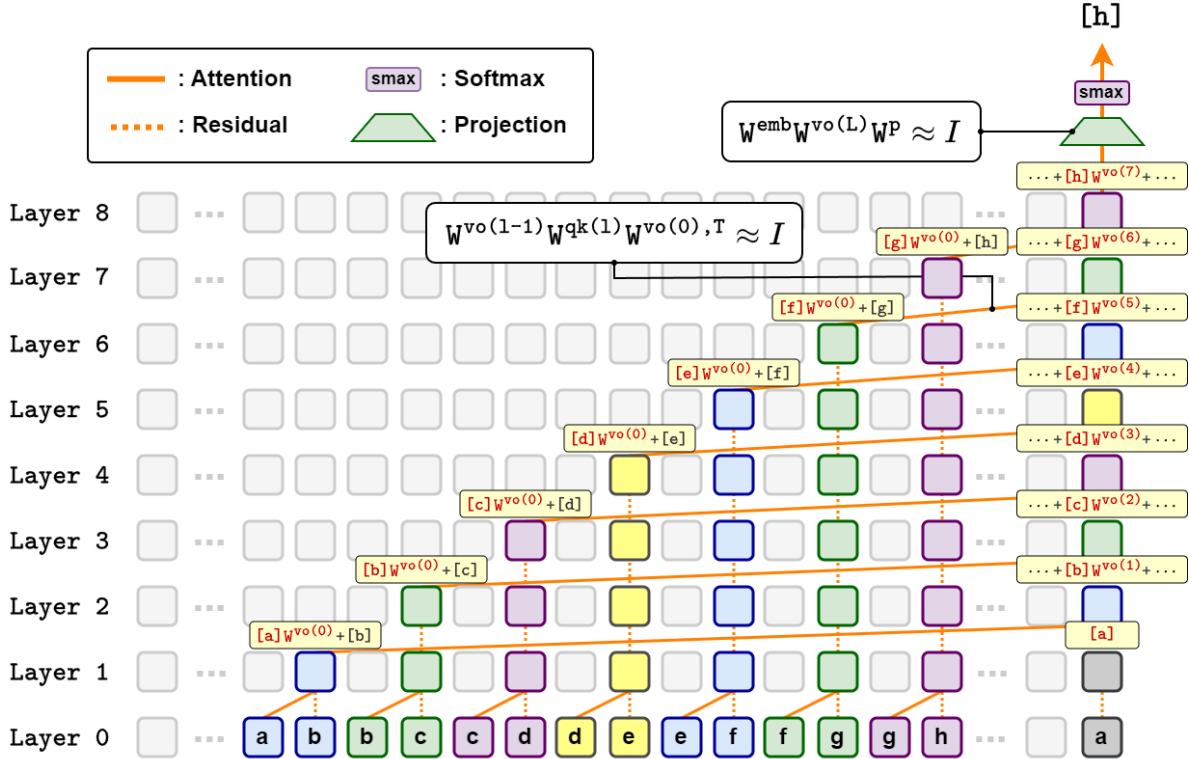

Figure 3: Illustration of how the Transformer model employs vertical thinking strategy for multi-step reasoning task.

It is important to note the distinction between information transmission triggered by attention and that induced by residual connections. In the attention mechanism, information [a] with dimension d_m is first mapped to a lower embedding dimension d_v through the matrix $\boldsymbol{W}^v$, and then it is projected back to d_m dimensions via the matrix $\boldsymbol{W}^o$. Consequently, the information [a] after passing through the attention layer becomes [a]$\boldsymbol{W}^{vo}$. In contrast, information transmitted through residual connections does not require additional processing; thus, after the first layer, the information at even indices transforms to [x$_{2i-1}$]$\boldsymbol{W}^{vo(0)}$ + [x$_{2i}$].

We observe that each token in Fig. 3 stores various information in various forms (projected by different matrices $\boldsymbol{W}^{vo(l)}$), which leads to a natural question: how does the attention layer effectively retrieve useful information while

avoiding interference from others? To address this question, we introduce the following lemma (the proof can be found in Appendix B):

Lemma 1. *Suppose token $\boldsymbol{x} = \sum_{i=1}^{n} \boldsymbol{a}_i \boldsymbol{W}_i \in \mathbb{R}^{d_m}$ and token $\boldsymbol{y} = \sum_{i=1}^{n} \boldsymbol{b}_i \boldsymbol{W}_i \in \mathbb{R}^{d_m}$, where $\boldsymbol{a}_i, \boldsymbol{b}_i \in \mathbb{R}^{d_m}$, $\boldsymbol{W}_i \in \mathbb{R}^{d_m \times d_m}$, $i = 1, 2, \cdots, n$. Each element of $\{\boldsymbol{a}_i\}_{i=1}^{n}$, $\{\boldsymbol{b}_i\}_{i=1}^{n}$ and $\{\boldsymbol{W}_i\}_{i=1}^{n}$ follows a normal distribution $\mathcal{N}(0, 1/d_m)$ and independent to others. Then, we have:*

$$\boldsymbol{x}\boldsymbol{W}_i^{\mathsf{T}} = \boldsymbol{a}_i + \mathcal{O}\left(\sqrt{\frac{n}{d_m}}\right), \quad \boldsymbol{y}\boldsymbol{W}_j^{\mathsf{T}} = \boldsymbol{b}_j + \mathcal{O}\left(\sqrt{\frac{n}{d_m}}\right), \tag{4}$$

$$\boldsymbol{x}\boldsymbol{W}_i^{\mathsf{T}}\boldsymbol{W}_j\boldsymbol{y}^{\mathsf{T}} = \boldsymbol{a}_i\boldsymbol{b}_j^{\mathsf{T}} + \mathcal{O}\left(\frac{n}{\sqrt{d_m}}\right). \tag{5}$$

It can be observed that the matrices $\{\boldsymbol{W}_i\}_{i=1}^{n}$ serve as a set of **buffers** for information. Each element of $\{\boldsymbol{a}_i\}_{i=1}^{n}$ is located in different buffers, and is almost unaffected by others. This property also applies for $\{\boldsymbol{b}_i\}_{i=1}^{n}$. By selecting the matrices associated with the relevant buffer, specific information contained in token $\boldsymbol{x}$ and token $\boldsymbol{y}$ can be extracted.

The concept of the buffer mechanism is useful for understanding the internal logic mechanisms of Transformer models. $\{\boldsymbol{W}^{q(l)}\}_{l=1}^{L}$ and $\{\boldsymbol{W}^{k(l)}\}_{l=1}^{L}$ can be viewed as "information extractors", while $\{\boldsymbol{W}^{vo(l)}\}_{l=1}^{L}$ can be considered as a set of buffers. We observe that in the final token of each reasoning layer, each new intermediate result is always associated with a new $\boldsymbol{W}^{vo}$. If these $\{\boldsymbol{W}^{vo(l)}\}_{l=1}^{L}$ matrices are mutually orthogonal or random, then these intermediate results can be regarded as being stored in a new buffer.

In each reasoning layer, the token at the last position contains the current intermediate result. Additionally, there exists a token that contains both the current intermediate result and the next step's reasoning result, with these stored in different buffers. The role of $\boldsymbol{W}^q$ and $\boldsymbol{W}^k$ is to extract the current intermediate results from these two tokens, enabling them to attend to each other due to having the same token. We refer to this feature as "*same-token matching*". To quantitatively characterize this property, we define the following match matrix:

$$h^{(l)}(\boldsymbol{X}) = (\boldsymbol{X}\boldsymbol{W}^{vo(l-1)})\boldsymbol{W}^{q(l)}\boldsymbol{W}^{k(l),\mathsf{T}}(\boldsymbol{X}\boldsymbol{W}^{vo(0)})^{\mathsf{T}} \tag{6}$$

$$= \boldsymbol{X}\boldsymbol{W}^{vo(l-1)}\boldsymbol{W}^{qk(l)}\boldsymbol{W}^{vo(0),\mathsf{T}}\boldsymbol{X}^{\mathsf{T}} \triangleq \boldsymbol{X}\,\mathrm{Ker}^{(l)}\,\boldsymbol{X}^{\mathsf{T}}, \, l \geq 2, \tag{7}$$

$$h^{(1)}(\boldsymbol{X}) = \boldsymbol{X}\boldsymbol{W}^{qk(1)}\boldsymbol{W}^{vo(0),\mathsf{T}}\boldsymbol{X}^{\mathsf{T}} \triangleq \boldsymbol{X}\,\mathrm{Ker}^{(1)}\,\boldsymbol{X}^{\mathsf{T}}. \tag{8}$$

where we temporarily ignore the effects introduced by the feedforward layers only in our analysis; a detailed version that includes the feedforward layers can be found in Appendix C. When same-token matching happens, the following should hold:

$$\mathrm{Ker}^{(l)} = \boldsymbol{W}^{vo(l-1)}\boldsymbol{W}^{qk(l)}\boldsymbol{W}^{vo(0),\mathsf{T}} \approx \boldsymbol{I}, \, l \geq 2 \tag{9}$$

$$\mathrm{Ker}^{(1)} = \boldsymbol{W}^{qk(1)}\boldsymbol{W}^{vo(0),\mathsf{T}} \approx \boldsymbol{I}, \tag{10}$$

$$h^{(l)}(\boldsymbol{X}_{tgt}) \approx \boldsymbol{X}_{tgt}\boldsymbol{X}_{tgt}^{T} = \boldsymbol{I} + \mathcal{O}\left(\frac{1}{\sqrt{d_m}}\right), \tag{11}$$

where we assume $\boldsymbol{X}_{tgt}$ remaining a random matrix with minimal changes during training. Eq.(9), Eq.(10), and Eq.(11) can explain why the model exhibits out-of-distribution generalization capability. Since the embedding vectors of token_OOD are untrained random vectors when the model's weights satisfy Eq.(9) and Eq.(10), then Eq.(11) automatically holds. This indicates that the model has learned the underlying patterns in the data.

3.1 Experiments

We utilized a 3-layer, single-head Transformer model to learn from a two-step reasoning dataset. Specific Experimental settings can be found in Appendix A. After training, the Transformer exhibits generalization capability in in-distribution (100% accuracy) and out-of-distribution data (over 82% accuracy).

Fig. 4 presents the experimental validation of Eq.(9) $\sim$ Eq.(11). We visualize the computed values of $h^{(1)}(\boldsymbol{X}_{tgt})$, $h^{(2)}(\boldsymbol{X}_{tgt})$, $\mathrm{Ker}^{(1)}$, and $\mathrm{Ker}^{(2)}$ with the model parameters after training. Notably, in the token_OOD region, token_OOD and $h^{(2)}(\boldsymbol{X}_{tgt})$ exhibit a diagonal structure similar to an identity matrix $\boldsymbol{I}$, ensuring the model's OOD generalization capability.

To establish a strong correlation between the model's OOD generalization and its ability to use the buffer mechanism for same-token matching, we define a metric for this capability, the matching score:

$$\text{Matching Score}(h^{(l)}) = \frac{1}{n}\mathbb{E}_{\boldsymbol{X}}\mathrm{Trace}(\sigma(h^{(l)}(\boldsymbol{X}))), \tag{12}$$

(a) $h^{(1)}(\mathbf{X}_{tgt})$

(b) $h^{(2)}(\mathbf{X}_{tgt})$

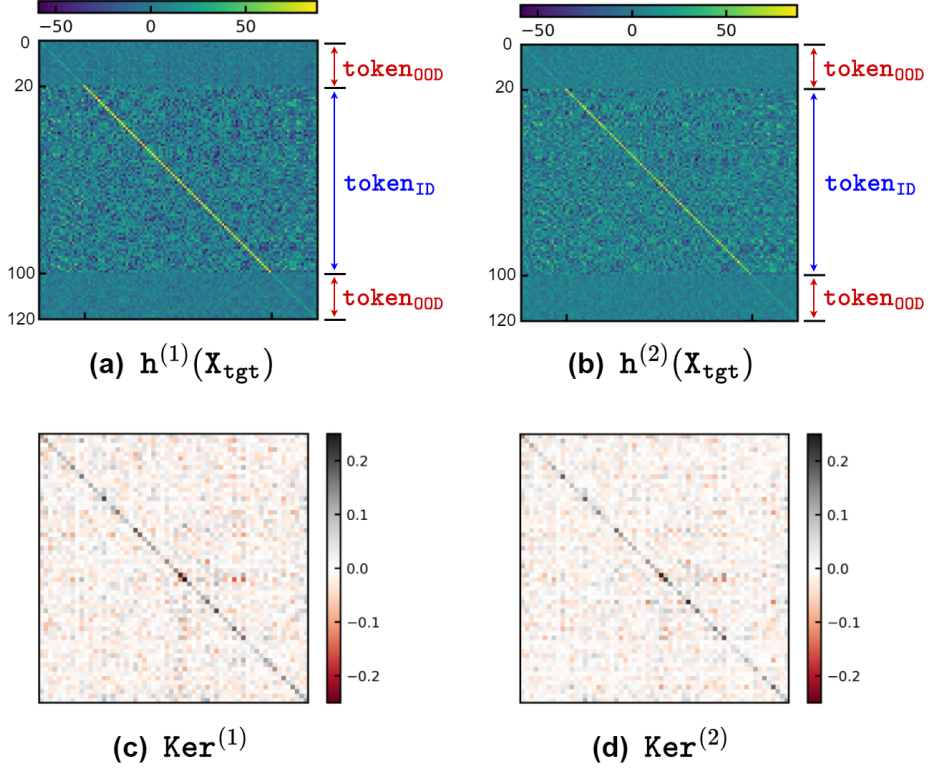**(c)** $\mathrm{Ker}^{(1)}$

(d) $\mathrm{Ker}^{(2)}$

Figure 4: (a) (b) Heatmap of $h^{(1)}(\mathbf{X}_{tgt})$ and $h^{(2)}(\mathbf{X}_{tgt})$. (c) (d) Heatmap of $\mathrm{Ker}^{(1)}$ and $\mathrm{Ker}^{(2)}$. For better presentation, we only plot $\mathrm{Ker}^{(1,2)}_{[:60,:60]}$ (the actual dimension of $\mathrm{Ker}^{(1,2)}$ is 400×400).

where $\mathbf{X} \in \mathbb{R}^{n \times d_m}$ is sampled from $\mathtt{token}_{\mathtt{ID}}$ or $\mathtt{token}_{\mathtt{OOD}}$ for expectation $\mathbb{E}_{\mathbf{X}}$, and σ takes the softmax operation. The level of diagonalization of $\mathrm{Ker}^{(l)}$ serves as the intrinsic driver for achieving same-token matching; thus, we also define a metric for this diagonalization level, the kernel score:

$$\text{Kernel Score}(\mathrm{Ker}^{(l)}) = \frac{n \cdot \text{Trace}(\mathrm{Ker}^{(l)})}{\sum_{i,j} \mathrm{Ker}^{(l)}_{i,j}}. \tag{13}$$

Fig. 5 illustrates the accuracy curve and the dynamic changes in the matching score and kernel score during training. It is observed that the increase in the model's ID and OOD generalization coincide with the increases in the model's matching score and kernel score. Based on the above experimental analysis, we conclude that the Transformer model indeed employs the buffer mechanism for vertical thinking.

According to the Buffer mechanism, in theory, by setting the model's weights in the following way, an L-layer model can achieve $(L-1)$-step reasoning *without the extra training process*:

$$\mathbf{W}^{q(0)} = \mathbf{W}^{q(1)} = I, \ \mathbf{W}^{q(l)} = \mathbf{W}^{vo(l-1),\mathsf{T}}, \ l \geq 2, \tag{14}$$

$$\mathbf{W}^{k(0)} = \sum_{i=1}^{[l_{\text{seq}}/2]} \mathbf{p}_{2i}\mathbf{p}_{2i-1}^{\mathsf{T}}, \ \mathbf{W}^{k(l)} = \mathbf{W}^{vo(0),\mathsf{T}}, \ l \geq 1, \tag{15}$$

where $\{\mathbf{W}^{vo(l)}\}_{l=1}^{L}$ are set as random matrices and the projection layer satisfies $\mathbf{W}^{p} = \mathbf{W}^{vo(L),\mathsf{T}}\mathbf{W}^{\text{emb},\mathsf{T}}$. Under this configuration, an 8-layer Transformer model can achieve 7-step reasoning (See Appendix C).

Another natural question is whether the model can still employ this mode of reasoning when the number of layers L is less than the number of reasoning steps. In fact, in this scenario, the model exhibits the ability to engage in parallel thinking. Specifically, the model can partition 2^L buffers through $\{\prod_{l \in J} \mathbf{W}^{vo(l)} | J \subset \{0, 1, \cdots, L-1\}\}$ since each $\prod_{l \in J} \mathbf{W}^{vo(l)}$ can be regarded as a new random matrix with the same distribution as $\mathbf{W}^{vo}$. We discuss this issue in detail in Appendix D.
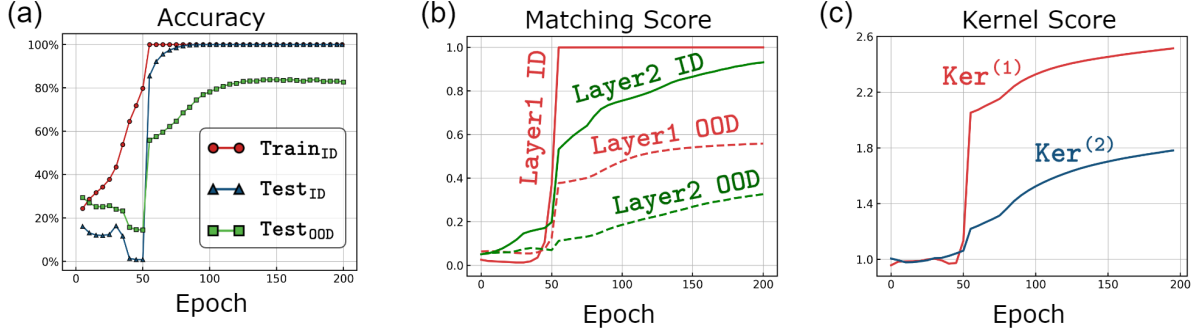
Figure 5: (a) Accuracy curve during training. (b) The dynamic evolution of the model's matching score. The red and blue lines represent the matching scores for the first and second layers, respectively. Solid and dashed lines indicate the matching scores when X is drawn from token_{ID} and $\text{token}_{\text{OOD}}$, respectively. (c) The kernel scores for the first (red) and second (blue) layers.

4 Understanding Horizontal Thinking Strategy With Buffer Mechanism

The Chain of Thought (CoT) approach, as a representative of horizontal thinking strategy, has become a prevalent mode of reasoning adopted by current large models, with numerous studies indicating that CoT can significantly enhance logical reasoning capability (Wei et al., 2022; Kojima et al., 2022). In this section, we will demonstrate that a Transformer model utilizing CoT can achieve arbitrary-step multi-step reasoning with only two layers. As shown in Fig. 6, we illustrate how the Transformer model employs CoT for multi-step reasoning. In the previously mentioned vertical thinking scenario, the model needed to allocate a new buffer $W^{vo(1)}$ for storing the intermediate result [b] and [c]. In contrast, with CoT, the model generates a new token to separately store the new intermediate information, effectively replacing the information [a] in the original buffer $W^{vo(0)}$ and I (identity matrix, which can also be treated as a buffer). Thus, CoT significantly enhances the model's information processing capability through buffer reuse.
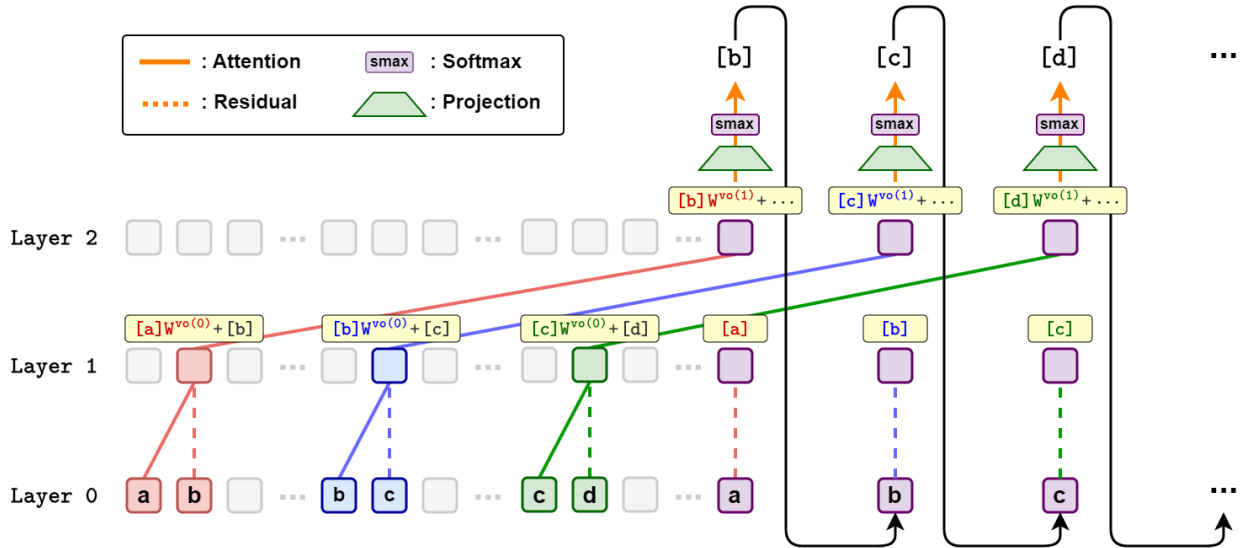

Figure 6: Illustration of how the Transformer model employs horizontal thinking strategy for multi-step reasoning task. The red, blue and green portions indicate the information activated during the first, second and third reasoning step, respectively.

7

5 Method for Improving Transformer's Data-Efficiency

In this section, we discuss how to improve data efficiency when employing the **vertical thinking strategy**, specifically, by enabling the model to learn the essence of logical reasoning with less data or training epoch. As mentioned in Section 3, this can be achieved by setting $\boldsymbol{W}^{vo(l-1),\mathsf{T}}\boldsymbol{W}^{qk(l)}\boldsymbol{W}^{vo(0),\mathsf{T}} \approx \boldsymbol{I}$.

A more intuitive approach is to replace $\boldsymbol{W}^{qk(l)}$ and $\boldsymbol{W}^{vo(l)}$ with $\boldsymbol{W}^{qk(l)} + \alpha^{(l)}I$ and $\boldsymbol{W}^{vo(l)} + \beta^{(l)}I$, where $\{\alpha^{(l)}\}_{l=1}^{L}$ and $\{\beta^{(l)}\}_{l=1}^{L}$ are learnable parameters. This Identity Matrix-Based Algorithm (denoted as IMBA) was first proposed in Boix-Adsera et al. (2023) and has been validated from both theoretical and empirical perspectives for its role in facilitating the model's learning of one-step reasoning data. However, in multi-step reasoning tasks, IMBA may lead to information interference. For instance, if $\boldsymbol{W}^{vo(l)}$ is replaced with $\boldsymbol{W}^{vo(l)} + \beta^{(l)}\boldsymbol{I}$, the storage representation of the two pieces of information transitions from [a]$\boldsymbol{W}^{vo}$+[b] to [a]$\boldsymbol{W}^{vo}$+($\beta^{(l)}$[a]+[b]), which introduces interference among the different pieces of information. Therefore, this approach may not be effective in enhancing the model's ability to perform multi-step reasoning.

Based on the understanding of buffer mechanism, we propose a **Random Matrix-Based Algorithm (RMBA)**, specifically by substituting $\boldsymbol{W}^{qk(l)}$ and $\boldsymbol{W}^{vo(l)}$ with $\boldsymbol{W}^{qk(l)} + \alpha^{(l)}\boldsymbol{Z}^{(l-1)}$ and $\boldsymbol{W}^{vo(l)} + \beta^{(l)}\boldsymbol{Z}^{(l)}$, where $\{\alpha^{(l)}\}_{l=1}^{L}$ and $\{\beta^{(l)}\}_{l=1}^{L}$ are learnable parameters and $\{\boldsymbol{Z}^{(l)}\}_{l=1}^{L}$ is a set of fixed random matrix following $N(0, 1/d_m)$. In this case, the information storage representation changes from [a]$\boldsymbol{W}^{vo}$+[b] to [a]$\boldsymbol{W}^{vo}$+[a]$\boldsymbol{Z}$+[b], effectively creating a new buffer.

Fig. 7 illustrates the different results of the two methods. The baseline is a three-layer transformer model, which fails to learn a two-step reasoning task with only 30,000 samples. Under various hyperparameter settings, when $\alpha_{\mathrm{ini}}^{(l)} \cdot \beta_{\mathrm{ini}}^{(l)} \geq 0$, the RMBA algorithm significantly enhances the model's generalization ability, while the IMBA shows no effect. This experiment validates our buffer mechanism understanding. This result also demonstrates that multi-step reasoning is not achieved by simply "stacking" multiple single-step reasonings. An algorithm that enhances single-step reasoning may not be applicable to multi-step reasoning. Therefore, investigating the mechanisms of multi-step reasoning is an important and meaningful topic.
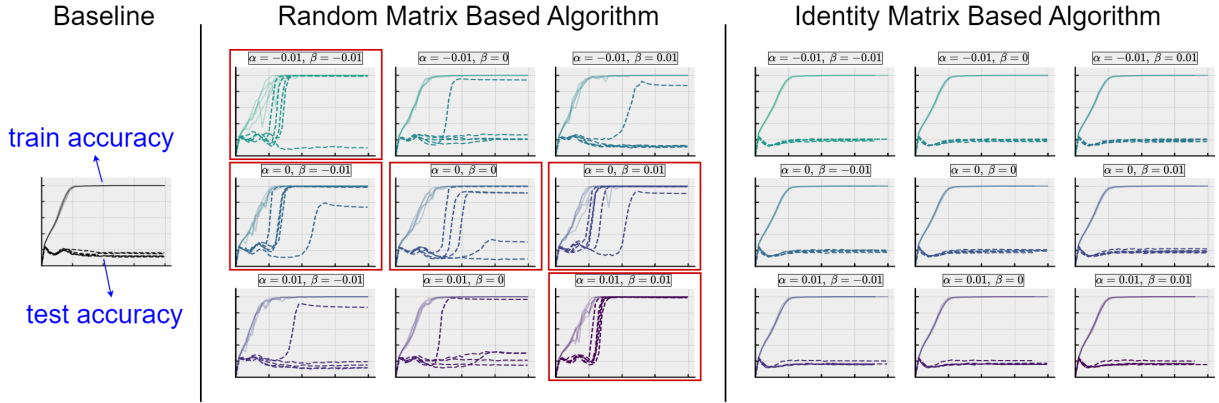

Figure 7: The impact of different learnable parameters' initial values, $\alpha^{(l)}$ and $\beta^{(l)}$, on the model's reasoning ability. When $\alpha_{\mathrm{ini}}^{(l)} = 0$ or $\alpha^{(l)}$ and $\beta^{(l)}$ have the same sign initially, the model's reasoning capability can be enhanced. The solid lines represent the training accuracy, while the dashed lines denote the test accuracy. Each experiment was conducted with 5 random seeds (each seed corresponds to one line). Detailed settings can be found in Appendix E.

5.1 Validation of Algorithm Performance on PrOntoQA Dataset

PrOntoQA dataset (Saparov & He, 2022) is constructed to test the reasoning capability of language models. We use the data generation procedure to create a 0.5M dataset of 3-step reasoning question-answer pairs, formatted as shown in Fig. 8(a).

We use a 12-layer, 12-head GPT-2 small model for this dataset. For the IMBA, we followed the settings provided in the open-source code (Boix-Adsera et al., 2023), which includes 144 learnable parameters $\alpha^{(l,h)}$ and 144 learnable parameters $\beta^{(l,h)}$. For RMBA, we replace $\boldsymbol{W}^{qk(l,h)}$ and $\boldsymbol{W}^{vo(l,h)}$ with $\boldsymbol{W}^{qk(l,h)} + \alpha^{(l,h)}\boldsymbol{Z}^{(l-1,h)}$ and $\boldsymbol{W}^{vo(l,h)} + \beta^{(l,h)}\boldsymbol{Z}^{(l,h)}$. Fig. 8(b) illustrates the impact of different algorithms on the performance of the original GPT-2 small

model (baseline) on this dataset. In this figure, accuracy reflects the model's precision in predicting True or False for the last token. The results indicate that the model utilizing RMBA achieves the highest data efficiency, reducing the number of iterations required to attain generalization by 75% compared to the baseline model.

To verify whether these algorithms enable the model to learn the essence of the reasoning process, we inserted several random tokens at random positions in each test sentence and recorded the accuracy of the different models. Fig. 8(b) shows the accuracy of each model outputting the correct answer as the number of random tokens increases. The IMBA models exhibit the least stability, while the RMBA models maintain the same level of stability as the baseline.

(a)

> Ex: Every sterpus is transparent. **Sterpuses are brimpuses.** Every sterpus is a lorpus. **Brimpuses are melodic.** Brimpuses are zumpuses. Each brimpus is a shumpus. Every shumpus is not fruity. Lorpuses are moderate. Gorpuses are metallic. Vumpuses are not melodic. Gorpuses are lempuses. Fae is a gorpus. **Fae is a sterpus.** Q: True or false: **Fae is not melodic.** A: False
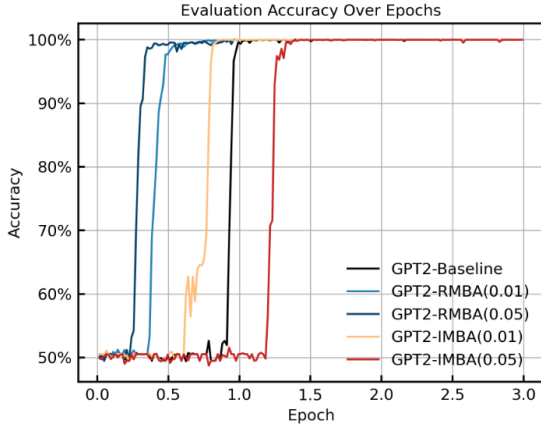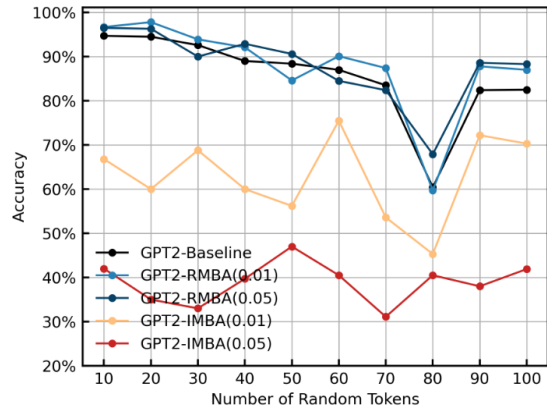
(b) (c)

Figure 8: (a) Example of PrOntoQA dataset. For each algorithm, we initialize the learnable parameter $\alpha^{(l)}, \beta^{(l)}$ at 0.01 and 0.05. (b) Accuracy curve of GPT-2 trained with RMBA and IMBA. (c) Stability of different GPT-2 models.

6 Related Work

Language model reasoning There have been numerous experimental and theoretical studies on language model reasoning. Abbe et al. (2022) examines the reasoning capabilities of neural networks using the Pointer Value Retrieval (PVR) benchmark, which was originally introduced in Zhang et al. (2021). Sharma et al. (2023) demonstrates that applying low-rank approximation of the certain weight layers to themselves can enhance reasoning performance across various tasks, and Chen et al. (2024a) explains this phenomenon in a two-layer Transformers model. Wang et al. (2024a) investigate both ID and OOD reasoning abilities on two synthetic tasks involving composition and comparison. Jiang et al. (2024) reveals that the reasoning process in Large Language Models (LLMs) is influenced by token bias and that these models continue to face challenges when dealing with more complex logical tasks. Abbe et al. (2024) introduces the distribution locality and shows Transformers require low locality. Zhang et al. (2024b); Luo et al. (2021); Zhou et al. (2022) shows that small initialization can facilitate model reasoning. Brinkmann et al. (2024) investigates the mechanism by which language models output intermediate reasoning paths in multi-step reasoning tasks.

Understanding the mechanism of neural model Our work builds upon previous studies on the attention mechanism (Voita et al., 2019; Vig, 2019; Kovaleva et al., 2019; Kobayashi et al., 2020). Numerous researchers have proposed various approaches to identify the roles of different heads in Transformers (Vig et al., 2020; Jeoung & Diesner, 2022; Wang et al., 2022; Conmy et al., 2023; Merullo et al., 2023; Guo et al., 2023; Wang & Weinan, 2024; Amsel et al., 2024; Li et al., 2024; Wang et al., 2024c). These methods predominantly employ the concept of perturbation. Similar to the observations made by Wang et al. (2023) and Dutta et al. (2024), who noted that large language models typically perform information aggregation in shallow layers and information induction in deeper layers, we have also observed comparable phenomena in our study. The idea of symbolic datasets is inspired by Poli et al. (2024); Zhang et al. (2024c). There have also been some insightful theoretical works on feedforward neural networks. A series of studies have

explored neural network preferences and generalization from the perspectives of regularization and frequency, etc. (Xu et al., 2019; Wang et al., 2024b; Jacot et al., 2018, 2020; Arora et al., 2019a, 2018). And Wu & Su (2023); Wang & Wu; Arora et al. (2022); Li et al. (2021); Wu et al. (2018); Zhu et al. (2018); Arora et al. (2019b) investigates the dynamical behavior of neural networks, while Ren et al. (2024) examines the factors influencing neural network generalization.

In-context learning and induction head Our work primarily investigates the model's ability to perform in-context learning. The concept of in-context learning (ICL) was first introduced by Brown et al. (2020). Since then, a series of studies have utilized induction heads to investigate ICL, yielding remarkable research outcomes (Olsson et al., 2022; Garg et al., 2022; Wang et al., 2022; Müller et al., 2021; Goldowsky-Dill et al., 2023; Bietti et al., 2024; Nichani et al., 2024; Edelman et al., 2024; Chen et al., 2024b; Todd et al., 2023; Chen & Zou, 2024). It is worth noting that induction heads can be considered as a special case of multi-step reasoning tasks with reasoning step equals to 1. However, multi-step reasoning is not a simple linear combination of single-step reasoning. In our work, we study the mechanism that enables multi-step reasoning, which has not been explored in previous studies.

7 Discussion

Conclusion. In this study, we investigated the buffer mechanism employed by Transformer models when performing multi-step reasoning using the vertical thinking strategy and horizontal thinking strategy. When utilizing the vertical thinking strategy, the model stores different intermediate results in separate buffers and transfers the reasoning results with same-token matching. In contrast, when applying the horizontal thinking strategy, the model reuses the existing buffers to store intermediate results, enabling reasoning over an arbitrary number of steps. We validated that the buffer mechanism is a key factor in enabling the model's ID and OOD generalization capabilities. Based on the buffer mechanism, we proposed a tailored approach, RMBA, to enhance the model's multi-step reasoning ability, significantly improving data efficiency when training GPT-2 on PrOntoQA datasets.

Limitations and Future Work. Our current work lacks in-depth theoretical analysis. In future work, we aim to conduct deeper theoretical modeling for multi-step reasoning problems and extend the buffer mechanism to other types of multi-step reasoning tasks.

References

Emmanuel Abbe, Samy Bengio, Elisabetta Cornacchia, Jon Kleinberg, Aryo Lotfi, Maithra Raghu, and Chiyuan Zhang. Learning to reason with neural networks: Generalization, unseen data and boolean measures. *Advances in Neural Information Processing Systems*, 35:2709–2722, 2022.

Emmanuel Abbe, Samy Bengio, Aryo Lotfi, Colin Sandon, and Omid Saremi. How far can transformers reason? the locality barrier and inductive scratchpad. *arXiv preprint arXiv:2406.06467*, 2024.

Noah Amsel, Gilad Yehudai, and Joan Bruna. On the benefits of rank in attention layers. *arXiv preprint arXiv:2407.16153*, 2024.

Sanjeev Arora, Nadav Cohen, Noah Golowich, and Wei Hu. A convergence analysis of gradient descent for deep linear neural networks. *arXiv preprint arXiv:1810.02281*, 2018.

Sanjeev Arora, Simon Du, Wei Hu, Zhiyuan Li, and Ruosong Wang. Fine-grained analysis of optimization and generalization for overparameterized two-layer neural networks. In *International Conference on Machine Learning*, pp. 322–332. PMLR, 2019a.

Sanjeev Arora, Simon S Du, Wei Hu, Zhiyuan Li, Russ R Salakhutdinov, and Ruosong Wang. On exact computation with an infinitely wide neural net. In *Advances in Neural Information Processing Systems*, pp. 8141–8150, 2019b.

Sanjeev Arora, Zhiyuan Li, and Abhishek Panigrahi. Understanding gradient descent on the edge of stability in deep learning. In *International Conference on Machine Learning*, pp. 948–1024. PMLR, 2022.

Alberto Bietti, Vivien Cabannes, Diane Bouchacourt, Herve Jegou, and Leon Bottou. Birth of a transformer: A memory viewpoint. *Advances in Neural Information Processing Systems*, 36, 2024.

Enric Boix-Adsera, Omid Saremi, Emmanuel Abbe, Samy Bengio, Etai Littwin, and Joshua Susskind. When can transformers reason with abstract symbols? *arXiv preprint arXiv:2310.09753*, 2023.

Jannik Brinkmann, Abhay Sheshadri, Victor Levoso, Paul Swoboda, and Christian Bartelt. A mechanistic analysis of a transformer trained on a symbolic multi-step reasoning task. *arXiv preprint arXiv:2402.11917*, 2024.

Tom Brown, Benjamin Mann, Nick Ryder, Melanie Subbiah, Jared D Kaplan, Prafulla Dhariwal, Arvind Neelakantan, Pranav Shyam, Girish Sastry, Amanda Askell, et al. Language models are few-shot learners. *Advances in neural information processing systems*, 33:1877–1901, 2020.

Lei Chen, Joan Bruna, and Alberto Bietti. How truncating weights improves reasoning in language models. *arXiv preprint arXiv:2406.03068*, 2024a.

Siyu Chen, Heejune Sheen, Tianhao Wang, and Zhuoran Yang. Training dynamics of multi-head softmax attention for in-context learning: Emergence, convergence, and optimality. *arXiv preprint arXiv:2402.19442*, 2024b.

Xingwu Chen and Difan Zou. What can transformer learn with varying depth? case studies on sequence learning tasks. *arXiv preprint arXiv:2404.01601*, 2024.

Arthur Conmy, Augustine Mavor-Parker, Aengus Lynch, Stefan Heimersheim, and Adrià Garriga-Alonso. Towards automated circuit discovery for mechanistic interpretability. *Advances in Neural Information Processing Systems*, 36: 16318–16352, 2023.

Alex Davies, Petar Veličković, Lars Buesing, Sam Blackwell, Daniel Zheng, Nenad Tomašev, Richard Tanburn, Peter Battaglia, Charles Blundell, András Juhász, et al. Advancing mathematics by guiding human intuition with ai. *Nature*, 600(7887):70–74, 2021.

Jacob Devlin, Ming-Wei Chang, Kenton Lee, and Kristina Toutanova. Bert: Pre-training of deep bidirectional transformers for language understanding. *arXiv preprint arXiv:1810.04805*, 2018.

Qingxiu Dong, Lei Li, Damai Dai, Ce Zheng, Zhiyong Wu, Baobao Chang, Xu Sun, Jingjing Xu, and Zhifang Sui. A survey on in-context learning. *arXiv preprint arXiv:2301.00234*, 2022.

Subhabrata Dutta, Joykirat Singh, Soumen Chakrabarti, and Tanmoy Chakraborty. How to think step-by-step: A mechanistic understanding of chain-of-thought reasoning. *arXiv preprint arXiv:2402.18312*, 2024.

Benjamin L Edelman, Ezra Edelman, Surbhi Goel, Eran Malach, and Nikolaos Tsilivis. The evolution of statistical induction heads: In-context learning markov chains. *arXiv preprint arXiv:2402.11004*, 2024.

Nelson Elhage, Neel Nanda, Catherine Olsson, Tom Henighan, Nicholas Joseph, Ben Mann, Amanda Askell, Yuntao Bai, Anna Chen, Tom Conerly, Nova DasSarma, Dawn Drain, Deep Ganguli, Zac Hatfield-Dodds, Danny Hernandez, Andy Jones, Jackson Kernion, Liane Lovitt, Kamal Ndousse, Dario Amodei, Tom Brown, Jack Clark, Jared Kaplan, Sam McCandlish, and Chris Olah. A mathematical framework for transformer circuits. *Transformer Circuits Thread*, 2021. https://transformer-circuits.pub/2021/framework/index.html.

Shivam Garg, Dimitris Tsipras, Percy S Liang, and Gregory Valiant. What can transformers learn in-context? a case study of simple function classes. *Advances in Neural Information Processing Systems*, 35:30583–30598, 2022.

Nicholas Goldowsky-Dill, Chris MacLeod, Lucas Sato, and Aryaman Arora. Localizing model behavior with path patching. *arXiv preprint arXiv:2304.05969*, 2023.

Tianyu Guo, Wei Hu, Song Mei, Huan Wang, Caiming Xiong, Silvio Savarese, and Yu Bai. How do transformers learn in-context beyond simple functions? a case study on learning with representations. *arXiv preprint arXiv:2310.10616*, 2023.

Arthur Jacot, Franck Gabriel, and Clément Hongler. Neural tangent kernel: Convergence and generalization in neural networks. *Advances in neural information processing systems*, 31, 2018.

Arthur Jacot, Berfin Simsek, Francesco Spadaro, Clément Hongler, and Franck Gabriel. Implicit regularization of random feature models. In *International Conference on Machine Learning*, pp. 4631–4640. PMLR, 2020.

Sullam Jeoung and Jana Diesner. What changed? investigating debiasing methods using causal mediation analysis. *arXiv preprint arXiv:2206.00701*, 2022.

Bowen Jiang, Yangxinyu Xie, Zhuoqun Hao, Xiaomeng Wang, Tanwi Mallick, Weijie J Su, Camillo J Taylor, and Dan Roth. A peek into token bias: Large language models are not yet genuine reasoners. *arXiv preprint arXiv:2406.11050*, 2024.

Goro Kobayashi, Tatsuki Kuribayashi, Sho Yokoi, and Kentaro Inui. Attention is not only a weight: Analyzing transformers with vector norms. *arXiv preprint arXiv:2004.10102*, 2020.

Takeshi Kojima, Shixiang Shane Gu, Machel Reid, Yutaka Matsuo, and Yusuke Iwasawa. Large language models are zero-shot reasoners. *Advances in neural information processing systems*, 35:22199–22213, 2022.

Olga Kovaleva, Alexey Romanov, Anna Rogers, and Anna Rumshisky. Revealing the dark secrets of bert. *arXiv preprint arXiv:1908.08593*, 2019.

Zhiyuan Li, Sadhika Malladi, and Sanjeev Arora. On the validity of modeling sgd with stochastic differential equations (sdes). *Advances in Neural Information Processing Systems*, 34:12712–12725, 2021.

Zhiyuan Li, Hong Liu, Denny Zhou, and Tengyu Ma. Chain of thought empowers transformers to solve inherently serial problems. *arXiv preprint arXiv:2402.12875*, 2024.

Peter J Liu, Mohammad Saleh, Etienne Pot, Ben Goodrich, Ryan Sepassi, Lukasz Kaiser, and Noam Shazeer. Generating wikipedia by summarizing long sequences. *arXiv preprint arXiv:1801.10198*, 2018.

Tao Luo, Zhi-Qin John Xu, Zheng Ma, and Yaoyu Zhang. Phase diagram for two-layer relu neural networks at infinite-width limit. *Journal of Machine Learning Research*, 22(71):1–47, 2021.

Jack Merullo, Carsten Eickhoff, and Ellie Pavlick. Circuit component reuse across tasks in transformer language models. *arXiv preprint arXiv:2310.08744*, 2023.

Samuel Müller, Noah Hollmann, Sebastian Pineda Arango, Josif Grabocka, and Frank Hutter. Transformers can do bayesian inference. *arXiv preprint arXiv:2112.10510*, 2021.

Eshaan Nichani, Alex Damian, and Jason D Lee. How transformers learn causal structure with gradient descent. *arXiv preprint arXiv:2402.14735*, 2024.

Catherine Olsson, Nelson Elhage, Neel Nanda, Nicholas Joseph, Nova DasSarma, Tom Henighan, Ben Mann, Amanda Askell, Yuntao Bai, Anna Chen, et al. In-context learning and induction heads. *arXiv preprint arXiv:2209.11895*, 2022.

OpenAI. Gpt-4 technical report, 2023.

Michael Poli, Armin W Thomas, Eric Nguyen, Pragaash Ponnusamy, Björn Deiseroth, Kristian Kersting, Taiji Suzuki, Brian Hie, Stefano Ermon, Christopher Ré, et al. Mechanistic design and scaling of hybrid architectures. *arXiv preprint arXiv:2403.17844*, 2024.

Alec Radford, Jeff Wu, Rewon Child, David Luan, Dario Amodei, and Ilya Sutskever. Language models are unsupervised multitask learners. 2019.

Gautam Reddy. The mechanistic basis of data dependence and abrupt learning in an in-context classification task. *arXiv preprint arXiv:2312.03002*, 2023.

Yinuo Ren, Chao Ma, and Lexing Ying. Understanding the generalization benefits of late learning rate decay. In *International Conference on Artificial Intelligence and Statistics*, pp. 4465–4473. PMLR, 2024.

Abulhair Saparov and He He. Language models are greedy reasoners: A systematic formal analysis of chain-of-thought. *arXiv preprint arXiv:2210.01240*, 2022.

Pratyusha Sharma, Jordan T Ash, and Dipendra Misra. The truth is in there: Improving reasoning in language models with layer-selective rank reduction. *arXiv preprint arXiv:2312.13558*, 2023.

Eric Todd, Millicent L Li, Arnab Sen Sharma, Aaron Mueller, Byron C Wallace, and David Bau. Function vectors in large language models. *arXiv preprint arXiv:2310.15213*, 2023.

Hugo Touvron, Thibaut Lavril, Gautier Izacard, Xavier Martinet, Marie-Anne Lachaux, Timothée Lacroix, Baptiste Rozière, Naman Goyal, Eric Hambro, Faisal Azhar, et al. Llama: Open and efficient foundation language models. *arXiv preprint arXiv:2302.13971*, 2023.

Trieu H Trinh, Yuhuai Wu, Quoc V Le, He He, and Thang Luong. Solving olympiad geometry without human demonstrations. *Nature*, 625(7995):476–482, 2024.

Ashish Vaswani, Noam Shazeer, Niki Parmar, Jakob Uszkoreit, Llion Jones, Aidan N Gomez, Łukasz Kaiser, and Illia Polosukhin. Attention is all you need. *Advances in neural information processing systems*, 30, 2017.

Jesse Vig. A multiscale visualization of attention in the transformer model. *arXiv preprint arXiv:1906.05714*, 2019.

Jesse Vig, Sebastian Gehrmann, Yonatan Belinkov, Sharon Qian, Daniel Nevo, Yaron Singer, and Stuart Shieber. Investigating gender bias in language models using causal mediation analysis. *Advances in neural information processing systems*, 33:12388–12401, 2020.

Elena Voita, David Talbot, Fedor Moiseev, Rico Sennrich, and Ivan Titov. Analyzing multi-head self-attention: Specialized heads do the heavy lifting, the rest can be pruned. *arXiv preprint arXiv:1905.09418*, 2019.

Boshi Wang, Xiang Yue, Yu Su, and Huan Sun. Grokked transformers are implicit reasoners: A mechanistic journey to the edge of generalization. *arXiv preprint arXiv:2405.15071*, 2024a.

Kevin Wang, Alexandre Variengien, Arthur Conmy, Buck Shlegeris, and Jacob Steinhardt. Interpretability in the wild: a circuit for indirect object identification in gpt-2 small. *arXiv preprint arXiv:2211.00593*, 2022.

Lean Wang, Lei Li, Damai Dai, Deli Chen, Hao Zhou, Fandong Meng, Jie Zhou, and Xu Sun. Label words are anchors: An information flow perspective for understanding in-context learning. *arXiv preprint arXiv:2305.14160*, 2023.

Mingze Wang and E Weinan. Understanding the expressive power and mechanisms of transformer for sequence modeling. *arXiv preprint arXiv:2402.00522*, 2024.

Mingze Wang and Lei Wu. A theoretical analysis of noise geometry in stochastic gradient descent. *arXiv preprint arXiv:2310.00692*.

Mingze Wang, Haotian He, Jinbo Wang, Zilin Wang, Guanhua Huang, Feiyu Xiong, Zhiyu Li, Lei Wu, et al. Improving generalization and convergence by enhancing implicit regularization. *arXiv preprint arXiv:2405.20763*, 2024b.

Xinyi Wang, Alfonso Amayuelas, Kexun Zhang, Liangming Pan, Wenhu Chen, and William Yang Wang. Understanding the reasoning ability of language models from the perspective of reasoning paths aggregation. *arXiv preprint arXiv:2402.03268*, 2024c.

Jason Wei, Xuezhi Wang, Dale Schuurmans, Maarten Bosma, Fei Xia, Ed Chi, Quoc V Le, Denny Zhou, et al. Chain-of-thought prompting elicits reasoning in large language models. *Advances in neural information processing systems*, 35:24824–24837, 2022.

Lei Wu and Weijie J Su. The implicit regularization of dynamical stability in stochastic gradient descent. In *International Conference on Machine Learning*, pp. 37656–37684. PMLR, 2023.

Lei Wu, Chao Ma, et al. How sgd selects the global minima in over-parameterized learning: A dynamical stability perspective. *Advances in Neural Information Processing Systems*, 31, 2018.

Zhi-Qin John Xu, Yaoyu Zhang, Tao Luo, Yanyang Xiao, and Zheng Ma. Frequency principle: Fourier analysis sheds light on deep neural networks. *arXiv preprint arXiv:1901.06523*, 2019.

Shunyu Yao, Dian Yu, Jeffrey Zhao, Izhak Shafran, Tom Griffiths, Yuan Cao, and Karthik Narasimhan. Tree of thoughts: Deliberate problem solving with large language models. *Advances in Neural Information Processing Systems*, 36, 2024.

Chiyuan Zhang, Maithra Raghu, Jon Kleinberg, and Samy Bengio. Pointer value retrieval: A new benchmark for understanding the limits of neural network generalization. *arXiv preprint arXiv:2107.12580*, 2021.

Yifan Zhang, Yang Yuan, and Andrew Chi-Chih Yao. On the diagram of thought. *arXiv preprint arXiv:2409.10038*, 2024a.

Zhongwang Zhang, Pengxiao Lin, Zhiwei Wang, Yaoyu Zhang, and Zhi-Qin John Xu. Initialization is critical to whether transformers fit composite functions by inference or memorizing. *arXiv preprint arXiv:2405.05409*, 2024b.

Zhongwang Zhang, Zhiwei Wang, Junjie Yao, Zhangchen Zhou, Xiaolong Li, Zhi-Qin John Xu, et al. Anchor function: a type of benchmark functions for studying language models. *arXiv preprint arXiv:2401.08309*, 2024c.

Hanxu Zhou, Qixuan Zhou, Zhenyuan Jin, Tao Luo, Yaoyu Zhang, and Zhi-Qin John Xu. Empirical phase diagram for three-layer neural networks with infinite width. *Advances in Neural Information Processing Systems*, 2022.

Zhanxing Zhu, Jingfeng Wu, Bing Yu, Lei Wu, and Jinwen Ma. The anisotropic noise in stochastic gradient descent: Its behavior of escaping from sharp minima and regularization effects. *arXiv preprint arXiv:1803.00195*, 2018.

A Experimental settings

In our experiments (Section 3), the vocabulary size is set to $d = 201$, and the hidden space dimension is set to $d_m = 400$ and $d_q = d_k = d_v = 64$. We use 200,000 2-step reasoning sequences (with sequence length equal to 13). The learning rate is set to 2e-5 and linearly warms up to 1e-4 within 400 epochs and then decays to 1e-5 within 3600 epochs. The batch size is set to 100. We use the AdamW optimizer with default parameters as set in PyTorch 2.3.0. We employ a gradient clipping strategy with `torch.nn.utils.clip_grad_norm_(model.parameters(), max_norm=1)`.

The experiments were conducted on a server with the following configuration:

- 64 AMD EPYC 7742 64-Core Processor.
- 256GB of total system memory.
- 2 NVIDIA A100 GPUs with 40GB of video memory each and 8 NVIDIA GeForce RTX 4080 GPUs with 16GB of video memory each.
- The experiments were run using the Ubuntu 22.04 LTS operating system.

The task shown above can be completed within 2 hours with a single NVIDIA A100 GPU. For other more complex examples, they can be finished within 24 hours.

B Proof of Lemma 1

Lemma 1 *Suppose token* $\boldsymbol{x} = \sum_{i=1}^{n} \boldsymbol{a}_i \boldsymbol{W}_i \in \mathbb{R}^{d_m}$ *and token* $\boldsymbol{y} = \sum_{i=1}^{n} \boldsymbol{b}_i \boldsymbol{W}_i \in \mathbb{R}^{d_m}$, *where* $\boldsymbol{a}_i, \boldsymbol{b}_i \in \mathbb{R}^{d_m}$, $\boldsymbol{W}_i \in \mathbb{R}^{d_m \times d_m}$, $i = 1, 2, \cdots, n$. *Each element of* $\{\boldsymbol{a}_i\}_{i=1}^{n}$, $\{\boldsymbol{b}_i\}_{i=1}^{n}$ *and* $\{\boldsymbol{W}_i\}_{i=1}^{n}$ *follows a normal distribution* $\mathcal{N}(0, 1/d_m)$ *and independent to others. Then, we have:*

$$\boldsymbol{x}\boldsymbol{W}_i^\mathsf{T} = \boldsymbol{a}_i + \mathcal{O}\left(\sqrt{\frac{n}{d_m}}\right), \quad \boldsymbol{y}\boldsymbol{W}_j^\mathsf{T} = \boldsymbol{b}_j + \mathcal{O}\left(\sqrt{\frac{n}{d_m}}\right), \tag{16}$$

$$\boldsymbol{x}\boldsymbol{W}_i^\mathsf{T}\boldsymbol{W}_j\boldsymbol{y}^\mathsf{T} = \boldsymbol{a}_i\boldsymbol{b}_j^\mathsf{T} + \mathcal{O}\left(\frac{n}{\sqrt{d_m}}\right). \tag{17}$$

Proof. We first show that $\boldsymbol{W}_i\boldsymbol{W}_j^\mathsf{T}$ (denoted as $\boldsymbol{Z}^{(i,j)}$) is also a random matrix with elements following a normal distribution $\mathcal{N}(0, 1/d_m)$ when $i \neq j$. In fact,

$$\mathbb{E}[(\boldsymbol{W}_i\boldsymbol{W}_j^\mathsf{T})_{s,t}] = \mathbb{E}[\sum_{k=1}^{d_m} (\boldsymbol{W}_i)_{sk}(\boldsymbol{W}_j)_{kt}] = \sum_{k=1}^{d_m} \mathbb{E}[(\boldsymbol{W}_i)_{sk}]\mathbb{E}[(\boldsymbol{W}_j)_{kt}] = 0,$$

$$\mathrm{Var}\left[(\boldsymbol{W}_i\boldsymbol{W}_j^\mathsf{T})_{s,t}\right] = \mathbb{E}\left[\left(\sum_{k=1}^{d_m}(\boldsymbol{W}_i)_{sk}(\boldsymbol{W}_j)_{kt}\right)^2\right]$$

$$= \sum_{k=1}^{d_m} \mathbb{E}\left[(\boldsymbol{W}_i)_{sk}^2\right]\mathbb{E}\left[(\boldsymbol{W}_j)_{kt}^2\right] = d_m \times (\frac{1}{d_m})^2 = \frac{1}{d_m},$$

which indicate $\{\boldsymbol{Z}^{(i,j)}\}$ follows the same distribution as $\{\boldsymbol{W}_i\}_{i=1}^{n}$. Therefore,

$$\mathbb{E}_{\{\boldsymbol{W}_j\}}\left[(\boldsymbol{x}\boldsymbol{W}_i^\mathsf{T})_t\right] = \sum_{j=1}^{n} \mathbb{E}_{\{\boldsymbol{Z}^{(j,i)}\}_j}\left[(\boldsymbol{a}_j\boldsymbol{Z}^{(j,i)})_t\right]$$

$$= \sum_{k=1}^{d_m} (\boldsymbol{a}_i)_k \mathbb{E}\left[(\boldsymbol{Z}^{(i,i)})_{kt}\right] + \sum_{\substack{j=1 \\ j \neq i}}^{n}\sum_{k=1}^{d_m} (\boldsymbol{a}_j)_k \mathbb{E}\left[(\boldsymbol{Z}^{(j,i)})_{kt}\right]$$

$$= \sum_{k=1}^{d_m} (\boldsymbol{a}_i)_k \mathbb{E}\left[(\boldsymbol{Z}^{(i,i)})_{kt}\right] = (\boldsymbol{a}_i)_t,$$

$$\mathrm{Var}_{\{\boldsymbol{W}_j\}}\left[(\boldsymbol{x}\boldsymbol{W}_i^{\mathsf{T}})_t\right] = \sum_{j=1}^{n}\mathrm{Var}_{\{\boldsymbol{Z}^{(j,i)}\}_j}\left[(\boldsymbol{a}_j\boldsymbol{Z}^{(j,i)})_t\right]$$

$$= \sum_{k=1}^{d_m}(\boldsymbol{a}_i)_k^2\mathrm{Var}\left[(\boldsymbol{Z}^{(i,i)})_{kt}\right] + \sum_{\substack{j=1\\j\neq i}}^{n}\sum_{k=1}^{d_m}(\boldsymbol{a}_j)_k^2\mathrm{Var}\left[(\boldsymbol{Z}^{(j,i)})_{kt}\right]$$

$$= \sum_{k=1}^{d_m}(\boldsymbol{a}_i)_k^2\mathrm{Var}\left[(\boldsymbol{Z}^{(i,i)})_{kt}\right] + \frac{1}{d_m}\sum_{\substack{j=1\\j\neq i}}^{n}\sum_{k=1}^{d_m}(\boldsymbol{a}_j)_k^2$$

$$= (\boldsymbol{a}_i)_t^2\mathrm{Var}\left[(\boldsymbol{Z}^{(i,i)})_{tt}\right] + \sum_{\substack{k=1\\k\neq t}}^{d_m}(\boldsymbol{a}_i)_k^2\mathrm{Var}\left[(\boldsymbol{Z}^{(i,i)})_{kt}\right] + \frac{1}{d_m}\sum_{\substack{j=1\\j\neq i}}^{n}\sum_{k=1}^{d_m}(\boldsymbol{a}_j)_k^2$$

$$= \frac{2}{d_m}(\boldsymbol{a}_i)_t^2 + \frac{1}{d_m}\sum_{\substack{k=1\\k\neq t}}^{d_m}(\boldsymbol{a}_i)_k^2 + \frac{1}{d_m}\sum_{\substack{j=1\\j\neq i}}^{n}\sum_{k=1}^{d_m}(\boldsymbol{a}_j)_k^2$$

$$= \frac{1}{d_m}(\boldsymbol{a}_i)_t^2 + \frac{1}{d_m}\sum_{j=1}^{n}\sum_{k=1}^{d_m}(\boldsymbol{a}_j)_k^2.$$

Therefore, $\mathrm{Var}\left[(\boldsymbol{x}\boldsymbol{W}_i^{\mathsf{T}})_t\right] = \mathrm{Var}_{\boldsymbol{a}}\left[\mathrm{Var}_{\{\boldsymbol{W}_j\}}\left[(\boldsymbol{x}\boldsymbol{W}_i^{\mathsf{T}})_t\right]\right] = n/d_m + 1/d_m^2$. And Chebyshev's inequality implies that $\boldsymbol{x}\boldsymbol{W}_i^{\mathsf{T}} = \boldsymbol{a}_i + \mathcal{O}\left(\sqrt{\frac{n}{d_m}}\right)$, which also holds for $\boldsymbol{y}\boldsymbol{W}_j^{\mathsf{T}}$.

Assume that $\boldsymbol{x}\boldsymbol{W}_i^{\mathsf{T}} = \boldsymbol{a}_i + \boldsymbol{z}_1$, $\boldsymbol{y}\boldsymbol{W}_j^{\mathsf{T}} = \boldsymbol{b}_j + \boldsymbol{z}_2$, $\boldsymbol{z}_1, \boldsymbol{z}_2$ are random vector with the elements follow the normal distribution $\mathcal{N}(n, 1/d_m)$, then,

$$\mathrm{Var}\left[\boldsymbol{x}\boldsymbol{W}_i^{\mathsf{T}}\boldsymbol{W}_j\boldsymbol{y}^{\mathsf{T}}\right] = \mathrm{Var}\left[\boldsymbol{a}_i\boldsymbol{b}_j^{\mathsf{T}} + \boldsymbol{a}_i\boldsymbol{z}_2^{\mathsf{T}} + \boldsymbol{z}_1\boldsymbol{b}_j^{\mathsf{T}} + \boldsymbol{z}_1\boldsymbol{z}_2^{\mathsf{T}}\right]$$

$$= d_m \times \frac{1}{d_m} \times \frac{1}{d_m} + 2 \times d_m \times \frac{1}{d_m} \times \frac{n}{d_m} + d_m \times \frac{n}{d_m} \times \frac{n}{d_m} = \frac{(n+1)}{d_m}.$$

Thus we have $\boldsymbol{x}\boldsymbol{W}_i^{\mathsf{T}}\boldsymbol{W}_j\boldsymbol{y}^{\mathsf{T}} = \boldsymbol{a}_i\boldsymbol{b}_j^{\mathsf{T}} + \mathcal{O}\left(\frac{n}{\sqrt{d_m}}\right)$. $\qquad\square$

C   Further Discussion on the Vertical Thinking Strategy

C.1   Information Fusion

In our symbolic dataset task, as mentioned in Section. 3, the first layer facilitates the fusion of token information at odd and even positions. We find that positional encoding plays a crucial role in the features of the first layer of attention. Fig. 9(a)(b) illustrates a comparison between the original attention mechanism and the positional attention mechanism calculated with eq. 18. As shown, there is minimal difference between the two approaches.

$$\mathcal{A}^{(0)}(\boldsymbol{X}^{\mathrm{pos}}) = \mathrm{softmax}\left(\frac{\mathrm{mask}(\boldsymbol{X}^{\mathrm{pos}}\boldsymbol{W}^{qk}\boldsymbol{X}^{\mathrm{pos},\mathsf{T}})}{\sqrt{d_k}}\right). \tag{18}$$

(a) $A^{(0)}(\mathbf{X_{tgt+pos}})$ **(b)** $A^{(0)}(\mathbf{X_{pos}})$
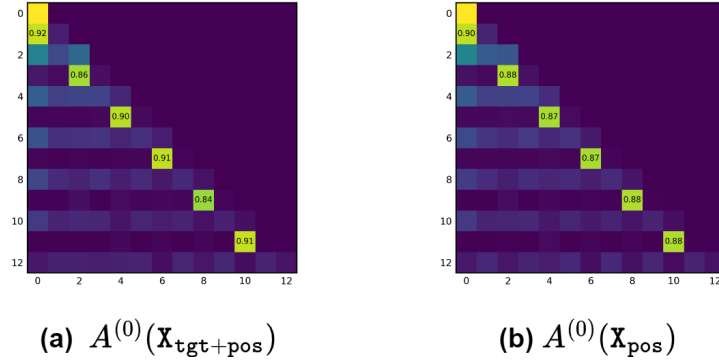
Figure 9: A comparison between the original attention (a) and the positional attention (b) of the first Transformer block, where $\boldsymbol{X}_{tgt+pos} = \boldsymbol{X}_{tgt} + \boldsymbol{X}_{pos}$.

C.2   Detailed Matching Matrix

In Section. 3, for simplicity of analysis, we ignored the impact of the feedforward layer. Here, we define a detailed version of the matching matrix as follows:

$$\tilde{h}^{(1)}(\boldsymbol{X}) = f^{(0)}(\boldsymbol{X})\boldsymbol{W}^{q(1),\mathsf{T}}[f^{(0)}(\boldsymbol{X}\boldsymbol{W}^{vo(0)})\boldsymbol{W}^{k(1),\mathsf{T}}]^{\mathsf{T}} \tag{19}$$

$$\tilde{h}^{(2)}(\boldsymbol{X}) = f^{(1)}[f^{(0)}(\boldsymbol{X})\boldsymbol{W}^{vo(1)}]\boldsymbol{W}^{q(2),\mathsf{T}}\left[f^{(1)} \circ f^{(0)}(\boldsymbol{X}\boldsymbol{W}^{vo(0)})\boldsymbol{W}^{k(2),\mathsf{T}}\right]^{\mathsf{T}}. \tag{20}$$

As shown in Fig. 10, the detailed matching matrices still maintain the diagonal element property in most cases, even for the out-of-distribution tokens.
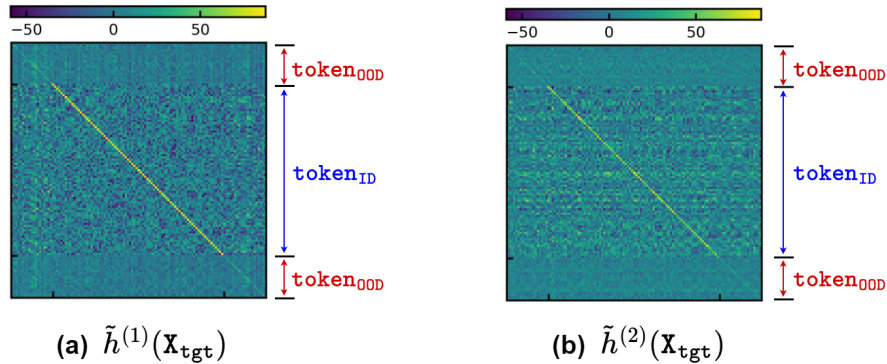

(a) $\tilde{h}^{(1)}(\mathbf{X_{tgt}})$ **(b)** $\tilde{h}^{(2)}(\mathbf{X_{tgt}})$

Figure 10: (a) Heatmap of $\tilde{h}^{(1)}(\boldsymbol{X}_{tgt})$ and $\tilde{h}^{(2)}(\boldsymbol{X}_{tgt})$. The diagonal elements exhibit the largest values, confirming the matching operation.

C.3 Weight Construction Method for Multi-Step Reasoning Networks

In Section. 3, we mentioned that by setting the weights in the following manner, we can enable an L-layer Transformer model to possess $(L-1)$-step reasoning capability.

$$\boldsymbol{W}^{q(0)} = \boldsymbol{W}^{q(1)} = I, \; \boldsymbol{W}^{q(l)} = \boldsymbol{W}^{vo(l-1),\mathsf{T}}, \; l \geq 2, \tag{21}$$

$$\boldsymbol{W}^{k(0)} = \sum_{i=1}^{[l_{\text{seq}}/2]} \boldsymbol{p}_{2i}\boldsymbol{p}_{2i-1}^{\mathsf{T}}, \; \boldsymbol{W}^{k(l)} = \boldsymbol{W}^{vo(0),\mathsf{T}}, \; l \geq 1, \tag{22}$$

where $\{\boldsymbol{W}^{vo(l)}\}_{l=1}^{L}$ are random matrices and the projection weight $\boldsymbol{W}^p = \boldsymbol{W}^{vo(L),\mathsf{T}}\boldsymbol{W}^{\text{emb},\mathsf{T}}$.

The specific construction method is as follows: To ensure that each buffer in the model has adequate robustness against interference, we set $d_m = d_q = d_k = d_v = 10000$. The feedforward layers are assigned zero weights so that the residual connection dominates. Since all the weight matrices we use are untrained random matrices, the layer normalization will have no effect. Fig. 11 shows the multi-step reasoning ability of an 8-layer Transformer. We tested natural order, reverse order, random order sentences, and sentences with inserted irrelevant tokens (i.e., token [20]), and the model was able to output the correct answer [8] in all cases. Each sentence begins with token [20] to prevent $\mathcal{A}_{0,0}^{(l)}$ always equals to 1, which could affect the buffer.

(a) natural order

(b) reverse order

(c) random order

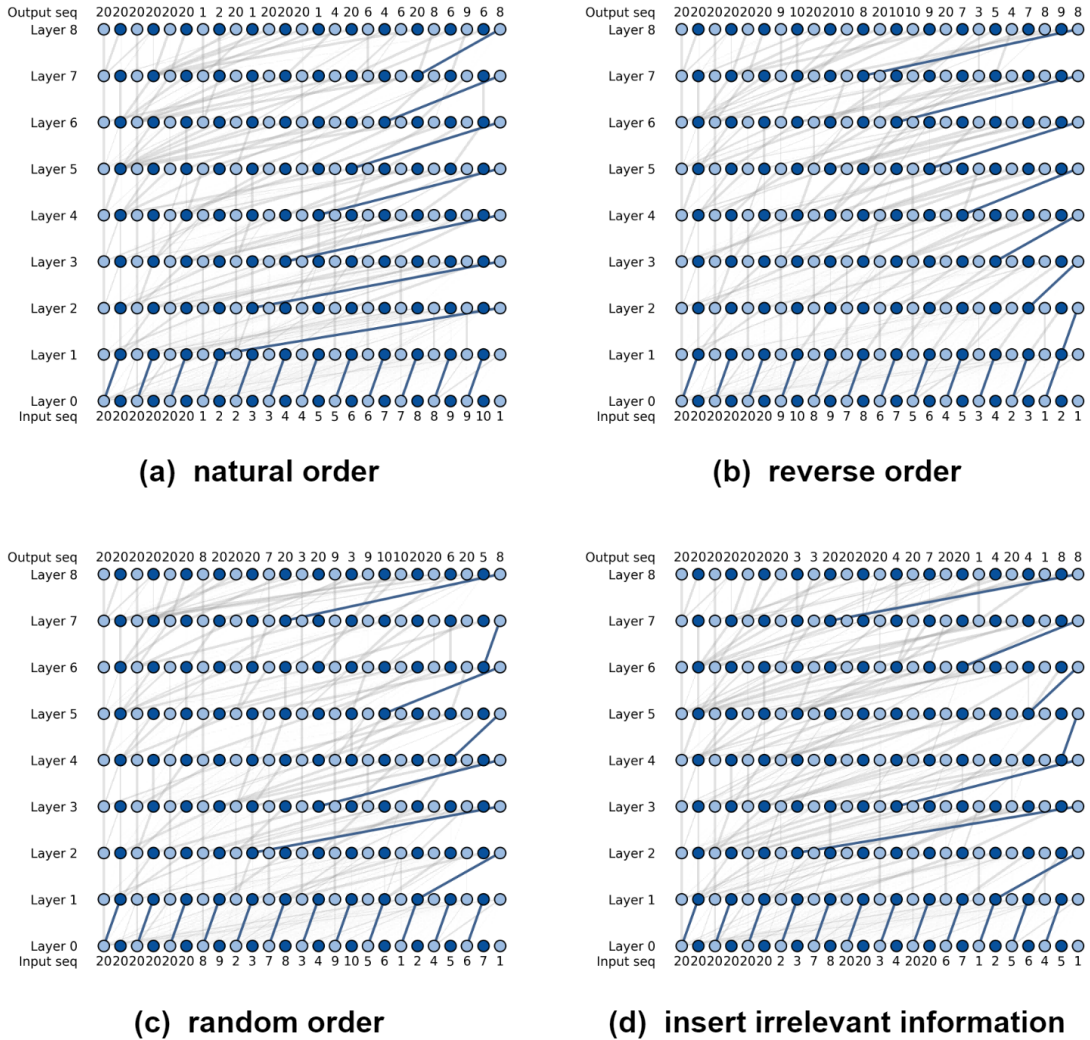(d) insert irrelevant information

Figure 11: The test results for the 8-layer Transformer we constructed. The gray lines represent attention values that do not affect the final outcome. The width of all lines is positively correlated with the attention weights.

D Mechanism of Parallel Reasoning

In this section, we investigate a natural question arising from Section 3: Can the model still perform reasoning through the vertical thinking strategy when the number of reasoning steps required by the task exceeds the number of reasoning layers? Our experimental studies reveal that, in such cases, the model exhibits a parallel reasoning strategy. Based on these observations, we hypothesize that the upper bound of the model's reasoning capability will grow exponentially with the depth of the model. We have conducted preliminary verification of this hypothesis using a simple program.

Mechanism of Parallel Reasoning. Fig. 12(a) illustrates the information flow of a 4-layer model completing 4-step reasoning. We observe that when the reasoning steps exceed or equal the number of model layers, the model performs reasoning parallelly in one layer. In the 2nd layer, different information undergoes two reasoning operations, enabling the subsequent three layers to achieve 4-step reasoning. Moreover, starting from the 2nd layer, the model's reasoning approach transits from matching tokens' values to matching tokens' positions. Token value matching is only utilized in the 1st layer.
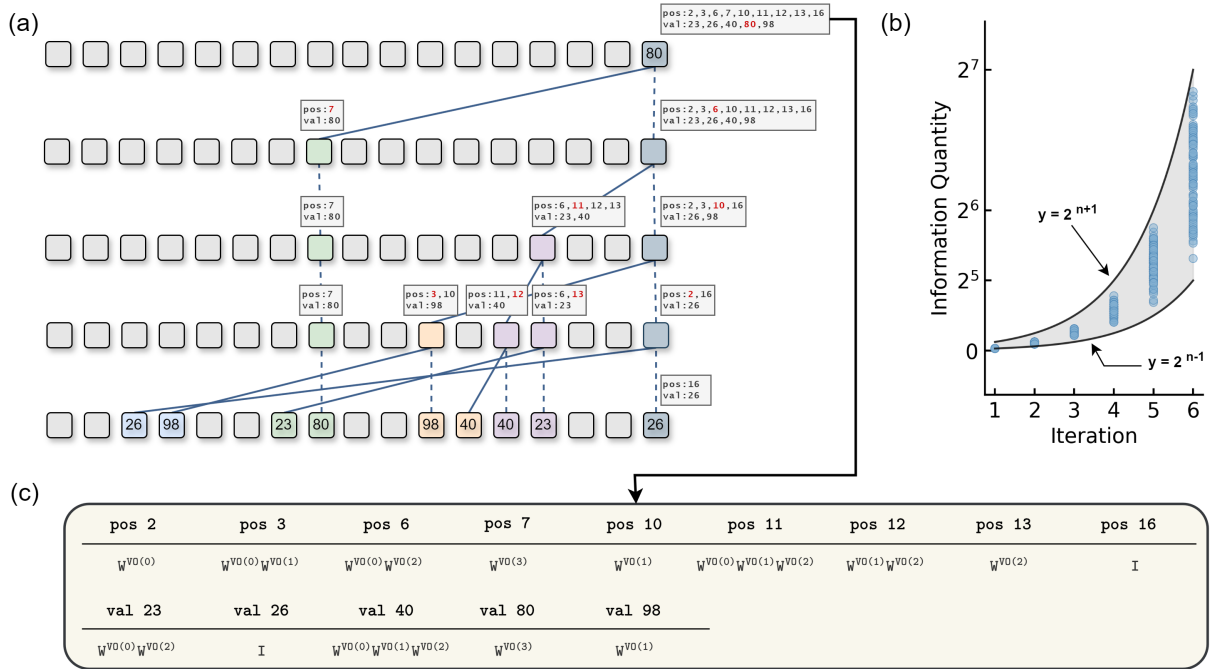

Figure 12: (a) Information flow of a 4-layer Transformer model completing 4-step reasoning. (b) Number of stored information tokens in the last position with respect to the number of iterations when propagating information based on the Info-Prop Rules. We randomly selected 1000 sentences for the simulation. The blue dots represent the simulation results. (c) The coefficients by which each information is multiplied.

Based on the mechanism of information propagation, at the l-th layer, if the information is transmitted through attention, it should be multiplied by a coefficient $\boldsymbol{W}^{vo(l)}$, whereas no such term is required if it is transmitted through residual connections. Consequently, in Fig. 12(c), we present the coefficients by which each information is multiplied. It is observed that for each positional information, the coefficients are distinct, and the same holds true for the value information. The variation in coefficients also indicates that the information is stored in different subspaces, thereby enabling parallel reasoning.

Upper Bound of Model's Reasoning Ability. Through the study of the buffer mechanism in Transformer models, we can estimate the upper bound of the reasoning ability for a general L-layer Transformer network. First, we assume that the model satisfies the following assumption.

Assumption 1. *Assume that the hidden space dimension d_m is sufficiently large, allowing different information to be stored in independent buffers with little interference. Moreover, information transmission is achieved solely through the same-token matching of the Attention module, without considering the influence of the feedforward module.*

We regard n tokens of a sequence as n nodes, each storing position and value information. The Transformer model follows the **Information Propagation (Info-Prop) Rules** (denoting the node transmitting information as i and the node receiving information as j, considering the existence of the attention mask, we require $i < j$):

- Rule 1: Odd positions can pass information to subsequent even positions, i.e., node i stores an odd number a in its position information, and node j stores $a + 1$ in its position information.
- Rule 2: The position information stored in node i and node j has common elements.
- Rule 3: The value information stored in node i and node j has common elements.

If any of the above three rules are satisfied, we consider that the information from node i can be transmitted to node j. When information transmission occurs, the position and value information stored in node j will take the union of the corresponding information from node i and node j.

Pseudocode 1 provides a detailed process of the Info-Prop Rules. Each `Node[i]` is a dictionary containing two attributes: pos (position) and val (value). `Node[i][pos]` and `Node[i][val]` are two sets. Initially, each set contains only its own information and will be updated according to the Info-Prop Rules. Fig. 12(b) shows the number of value information stored in the last token with respect to the number of iterations under our set of rules. It can be observed that the stored information exhibits an approximately exponential growth pattern with the number of iterations.

Algorithm 1 Information Propagation Rules

1: Initialize an empty dictionary Node
2: **for** each token i in the sequence **do**
3:    `Node[i][pos]` ← i
4:    `Node[i][val]` ← token i
5: **end for**
6: `Node_new` ← Node
7: Information propagation
8: **for** each node i in Node **do**
9:    **for** each node j > i in Node **do**
10:      rule1 ← any even number $a \in$ `Node[i][pos]` satisfies $a + 1 \in$ `Node[j][pos]`
11:      rule2 ← `Node[i][val]` $\cap$ `Node[j][val]` $\neq \varnothing$
12:      rule3 ← `Node[i][pos]` $\cap$ `Node[j][pos]` $\neq \varnothing$
13:      **if** rule1 or rule2 or rule3 **then**
14:        `Node_new[j][pos]` ← `Node_new[j][pos]` $\cup$ `Node[i][pos]`
15:        `Node_new[j][val]` ← `Node_new[j][val]` $\cup$ `Node[i][val]`
16:      **end if**
17:    **end for**
18: **end for**

A possible explanation for this experimental result is that in the L-th layer, the buffers of the Transformer can be represented as $\{\prod_{l \in J} \boldsymbol{W}^{vo(l)} | J \subset \{0, 1, \cdots, L - 1\}\}$. Therefore, the maximum amount of information (target information and position information) in the last layer is 2^{L+1}. In practice, the hidden space dimensions d_m, d_q, d_k, and d_v of large language models are far from meeting the requirements of Assumption 1. Consequently, the actual reasoning ability of large language models is constrained by the hidden space dimensions.

E   Details for RMBA Experiment

This section provides supplementary details on the experimental setup for the RMBA experiment. We use a 3-layer single-head Transformer with $d_q = d_k = d_v = 64$ and $d_m = 400$. The training set consists of 30,000 2-step reasoning chains. We trained the model for 200 epochs in total. In this setting, the Transformers have poor generation ability even in the in-distribution test dataset.

We replace $W^{qk(l)}$ and $W^{vo(l)}$ with $W^{qk(l)} + \alpha^{(l)}Z^{(l-1)}$ and $W^{vo(l)} + \beta^{(l)}Z^{(l)}$, respectively, where $\alpha^{(l)}$ and $\beta^{(l)}$ are learnable parameters, and $\{Z^{(l)}\}_{l=1}^L$ is a set of random matrix following $N(0, 1/d_m)$. Therefore, 6 extra learnable parameters are added to this 3-layer single-head model in total. Fig. 13 and Fig. 14 show the loss and accuracy of the Transformer under different settings. Fig. 15 shows the changes of the learnable parameters $\alpha^{(l)}$ and $\beta^{(l)}$ during training.
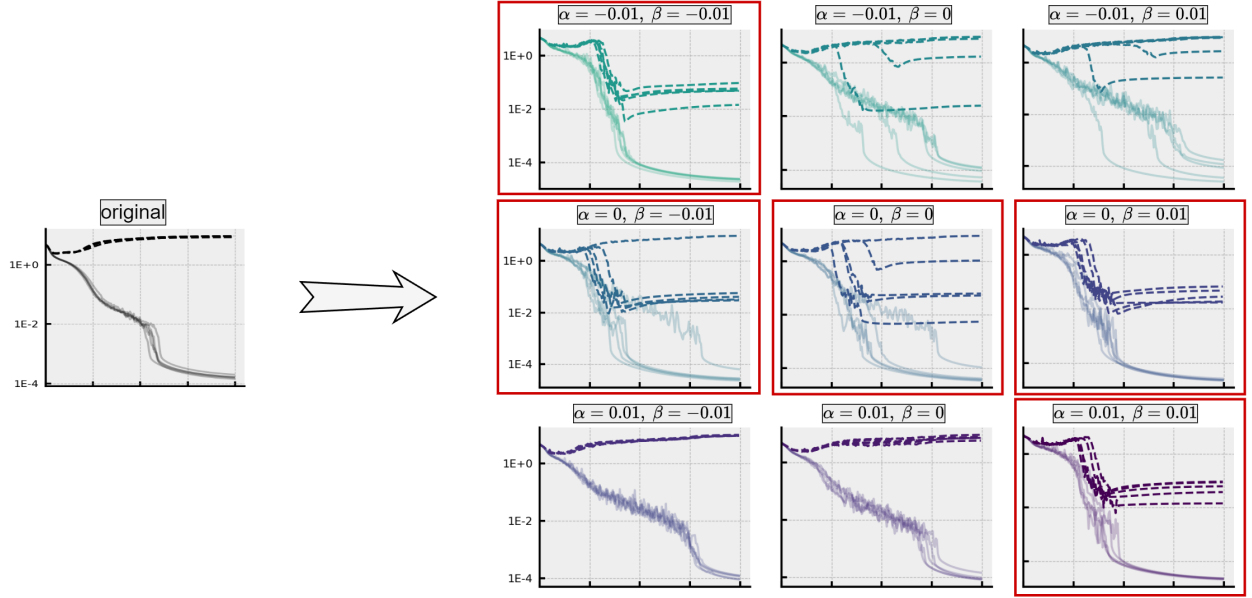

Figure 13: The impact of different learnable parameters' initial values, $\alpha^{(l)}$ and $\beta^{(l)}$, on the model's reasoning ability. The solid lines represent the training loss, while the dashed lines denote the test loss. Each experiment was conducted with 5 random seeds.
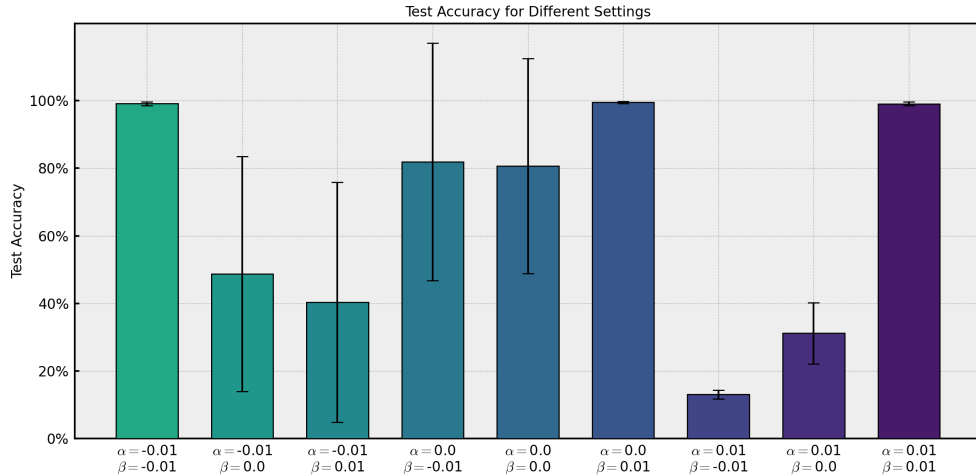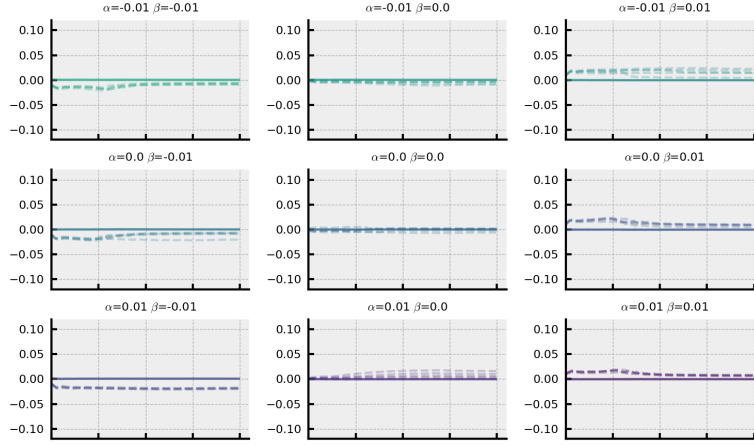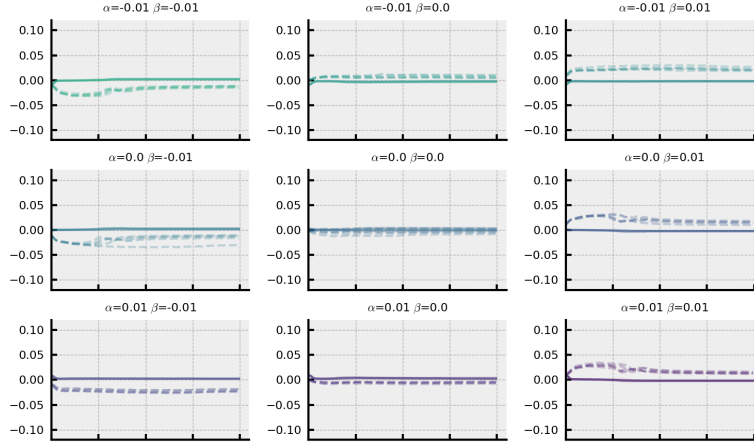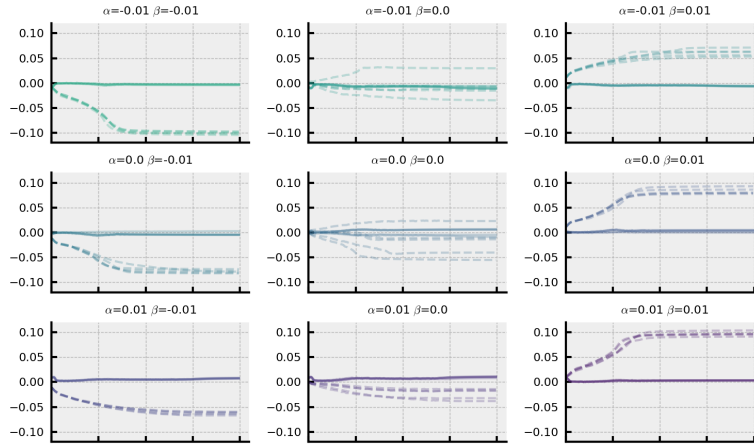

Figure 14: The average accuracy of different initial value of $\alpha^{(l)}$ and $\beta^{(l)}$.

(a) layer 0

(b) layer 1

(c) layer 2

Figure 15: Changes of the learnable parameters $\alpha^{(l)}$ and $\beta^{(l)}$ during training. The solid lines represent the $\alpha^{(l)}$, while the dashed lines denote the $\beta^{(l)}$. Each experiment was conducted with 5 random seeds.